

## Structure and hyperfine parameters of cyclopropyl and bicyclobutyl radicals from postHartree–Fock computations

Vincenzo Barone and Robert Subra

Citation: *J. Chem. Phys.* **104**, 2630 (1996); doi: 10.1063/1.470987

View online: <http://dx.doi.org/10.1063/1.470987>

View Table of Contents: <http://jcp.aip.org/resource/1/JCPSA6/v104/i7>

Published by the AIP Publishing LLC.

---

### Additional information on J. Chem. Phys.

Journal Homepage: <http://jcp.aip.org/>

Journal Information: [http://jcp.aip.org/about/about\\_the\\_journal](http://jcp.aip.org/about/about_the_journal)

Top downloads: [http://jcp.aip.org/features/most\\_downloaded](http://jcp.aip.org/features/most_downloaded)

Information for Authors: <http://jcp.aip.org/authors>

## ADVERTISEMENT



**Goodfellow**  
metals • ceramics • polymers • composites  
70,000 products  
450 different materials  
small quantities *fast*

[www.goodfellowusa.com](http://www.goodfellowusa.com)

# Structure and hyperfine parameters of cyclopropyl and bicyclobutyl radicals from post-Hartree–Fock computations

Vincenzo Barone<sup>a)</sup>

*Dipartimento di Chimica, Università Federico II, via Mezzocannone 4, I-80134 Napoli, Italy*

Robert Subra

*Laboratoire d'Etudes Dynamiques et Structurales de la Selectivite (LEDSS). Universite Joseph Fourier, BP53X, F-38041 Grenoble Cedex, France*

(Received 9 October 1995; accepted 3 November 1995)

Extensive post-Hartree–Fock calculations are reported for the geometrical structures and hyperfine parameters of cyclopropyl and bicyclobutyl radicals. Computations for the parent molecules, whose structures are experimentally well characterized, show that reliable geometrical parameters are obtained, especially for bicyclobutane, only when using sufficiently flexible basis sets including *f* functions on carbon. Isotropic hyperfine splittings obtained by purposely tailored basis sets, proper treatment of correlation, and inclusion of vibrational averaging effects are in remarkable agreement with experiment. Our results suggest a revision of the accepted assignment for bicyclobutyl radical and suggest that long-range couplings are not governed by the well-known *W* rule but rather by a syn rule. © 1996 American Institute of Physics. [S0021-9606(96)03006-0]

## I. INTRODUCTION

Organic free radicals are generally shortly lived, highly reactive species, and the means of experimentally determining their structures and properties are therefore fairly limited. The most successful approaches are based on the determination of the hyperfine splittings (hfs), in magnitude and sign, in relation to the geometry of the radical under consideration. In recent years a renewed interest for these problems has arisen from the finding of the role played by some radical species in proteins and nucleic acids,<sup>1–4</sup> by the effectivity of spin probes to study biological materials,<sup>5–8</sup> and from the use of organic free radicals as building blocks in molecular magnetic materials.<sup>9,10</sup> Several experimental studies have provided a large amount of spectroscopic data, but interpretation of the results in structural terms is often difficult. As a consequence there is a need for the development and validation of well defined computational protocols including reliable electronic methods and proper treatment of vibrational averaging effects arising from large amplitude nuclear motions.

As far as localized radicals are concerned, the features of hyperfine parameters are strongly dependent on the geometrical and topological relationships between the various nuclei and the localized orbital nominally containing the unpaired electron.<sup>11–13</sup> In this context radicals with a rigid skeleton are interesting because averaging between different conformations does not occur and only local vibrational effects are operative.<sup>14</sup> Furthermore some radicals belonging to this class are characterized by significant long-range couplings, which are usually negligible.<sup>15–18</sup> On the other hand, rigid backbones often induce significant strain and unusual electronic structures, which, in turn, represent a particularly severe benchmark for quantum mechanical methods. As a consequence we decided to perform a comprehensive study of

cyclopropyl and bicyclobutyl radicals together with their parent molecules. Together with their intrinsic interest, these systems are small enough to be studied by the most refined post Hartree–Fock methods,<sup>19–23</sup> thus allowing a reliable validation of cheaper approaches, which become unavoidable for the more interesting large free radicals.<sup>24</sup>

## II. THE METHOD

Electronic computations have been performed with the GAUSSIAN 92 code<sup>25</sup> and vibrational studies by the DiNa package.<sup>26,27</sup>

Electronic wave functions were generated by the UHF formalism, correlation energy then being introduced by second-order many-body perturbation theory (UMP2) or by the so-called quadratic CI approach including single and double excitations (UQCISD).<sup>28</sup> Properties were computed analytically by the relaxed density approach<sup>19(b)</sup> including all the electrons in the correlation treatment. Although the wave function consisting of UHF orbitals does not represent a correct spin state, all the computations reported in the present study give  $\langle S^2 \rangle < 0.760$ , and annihilation of the quartet contribution leaves no residual spin contamination. In such circumstances we can expect good structures and spin dependent properties from unrestricted computations.

Recent work shows that, at least for carbon centered  $\pi$  and quasi- $\pi$  radicals, UMP2 spin densities at nuclei are close to those obtained by more sophisticated approaches.<sup>14,19(a),29,30</sup> Furthermore, the popular Huzinaga–Dunning polarized double- $\zeta$  basis set<sup>31–33</sup> (hereafter DZP) is often quite adequate for the study of structures and magnetic properties.<sup>14,29,30</sup> As a consequence, the structures of the most significant conformers have been fully optimized by gradient methods at the UMP2/DZP level. Next saturation of the basis set with respect to geometrical structures has been investigated using a triple- $\zeta$  contraction of *p* orbitals, double

<sup>a)</sup>Corresponding author.

TABLE I. Geometrical parameters (Å and degrees) for cyclopropane and bicyclobutane. See Fig. 1 for the atom labeling.

Cyclopropane				Bicyclobutane			
Parameter	UMP2/DZP	UMP2/TZ2Pf	Expt.	Parameter	UMP2/DZP	UMP2/TZ2Pf	Expt.
CC	1.515	1.504	1.512	C1C2	1.518	1.497	1.497±0.003
CH	1.084	1.079	1.083	C1C3	1.503	1.495	1.498±0.004
HCH	115.10	115.00	114.0	C1H1	1.078	1.074	1.071±0.004
				C2H21	1.087	1.083	1.093±0.008
				C2H22	1.090	1.087	1.093±0.008
				C1C2C3	60.23	60.11	59.97
				C1C3H31	126.37	127.82	128.37
				H21C2H22	114.91	115.05	115.57
				(C1C2C3)(C1C4C3)	122.70	121.66	121.67
				(C2H21)(C1C2C3)	123.68	123.33	122.87
				(C2H22)(C1C2C3)	121.40	121.61	121.57

sets of polarization functions on all atoms, and a single set of  $f$  functions on each carbon atom.<sup>34</sup> This basis set will be referred to as TZ2Pf.

Only isotropic hyperfine splittings (hfs)  $a_N$  are considered here. They are related to the spin densities at the corresponding nuclei by

$$a_N = \frac{8\pi}{3} \beta_e g_N \beta_N \sum_{\mu, \nu} P_{\mu, \nu}^{\alpha-\beta} \langle \varphi_\mu | \delta(\mathbf{r}_{kN}) | \varphi_\nu \rangle.$$

Reliable values of this property can be computed by single-point computations with the (10,6,1;5,1)/[6,4,1;3,1] set introduced by Chipman<sup>35</sup> and further validated in Ref. 30 (referred to as TZP<sup>+</sup> basis set<sup>30</sup>). Finally saturation of correlation contributions for relative stabilities of different energy minima, inversion barriers, and isotropic hfs has been investigated by single point UQCISD/DZP and UQCISD/TZP<sup>+</sup> computations.

The study of large amplitude vibrations requires, especially in the case of large molecules, some separation between the active large amplitude motion (LAM) and the *spectator* small amplitude modes (SAM).<sup>36,37</sup> For intramolecular dynamics, description of the LAM in terms of the so-called distinguished coordinate (DC) approach has the advantage of being invariant upon isotopic substitutions and also well defined beyond energy minima. This model corresponds to the construction of the one-dimensional path through the optimization of all the other geometrical parameters at selected values of a specific internal coordinate. Successive points coming from separate geometry optimizations (as is the case for the DC model) introduce the problem of their relative orientation. In fact, the distance in mass weighted Cartesian coordinates between adjacent points is altered by the rotation or translation of their respective reference axes. The problem of translations has the trivial solution of centering the reference axes at the center of mass of the system. On the other hand, for nonplanar systems, the problem of rotations does not have an analytical solution and must be solved by numerical minimization of the distance between successive points as a function of the Euler angles of the system.<sup>38</sup>

The successive step consists in determining vibrational eigenvalues and eigenfunctions. Local basis set methods are tailored to this end since they give reliable results independently on the shape of the profile. Cubic splines were used to interpolate the potential along the LAP and to generate a larger set of equispaced points on which cubic splines were used as basis functions.<sup>39</sup> The expectation value  $\langle O \rangle_j$  of a given observable in the vibrational eigenstate  $|j\rangle$  corresponding to the eigenvalue  $\epsilon_j$  is given by

$$\langle O \rangle_j = O_{\text{ref}} + \langle j(s) | \Delta O(s) | j(s) \rangle,$$

where  $O_{\text{ref}}$  is the value of the observable at the reference configuration, and  $\Delta O(s)$  is the expression (here a spline fit) giving its variation as a function of the progress variable  $s$ . The temperature dependence of the observable is obtained by assuming a Boltzmann population of the vibrational levels, so that

$$\langle O \rangle_T = O_{\text{ref}} + \frac{\sum_{j=0}^{\infty} \langle j | \Delta O | j \rangle \exp[(\epsilon_0 - \epsilon_j)/KT]}{\sum_{j=0}^{\infty} \exp[(\epsilon_0 - \epsilon_j)/KT]}.$$

The above equations point out the possibility of computing the reference value of the observable at a very sophisticated level (QCISD/TZP<sup>+</sup> in our protocol) and vibrational averaging effects at a lower level (UMP2/DZP in our protocol).

### III. RESULTS AND DISCUSSION

In order to evaluate the reliability of our computational procedure, we have performed a preliminary investigation of the structures of the parent molecules cyclopropane and bicyclo[1.1.0]butane (hereafter referred to simply as bicyclobutane), which are well characterized.<sup>40–43</sup>

In the case of cyclopropane (Table I), the geometrical parameters computed at the MP2 level are in fair agreement with experiment. The only significant effect of basis set extension is a shortening of the CC bond length, with the values obtained by the two basis sets enclosing the experimental one. The same effect is found for bicyclobutane (Fig. 1 and Table I), but in this case only the TZ2Pf basis set is able to reproduce the equal values of all the CC bond lengths evidenced by experiment. At this level all the geometrical pa-

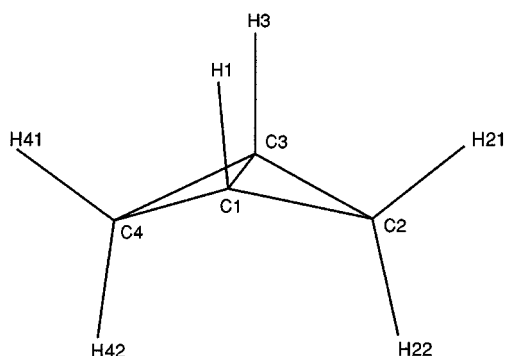


FIG. 1. Structure and atom labeling for bicyclo[1.1.0]butane.

rameters are within the error bar of the experimental determination. As a matter of fact the agreement is much improved with respect to previous computations employing Hartree–Fock and MC-SCF approaches with medium size basis sets.<sup>44,45</sup>

In the case of cyclopropyl radical (Fig. 2) we have performed full geometry optimizations both for the  $C_s$  equilibrium structure and the  $C_{2v}$  transition state governing inversion at the radical center. In the case of bicyclo[1.1.0]butane we have considered only the radical obtained by removing a hydrogen atom from a methylene group (hereafter referred to simply as bicyclobutyl radical). Full geometry optimization have been performed for *exo* (Fig. 3) and *endo* (Fig. 4) equilibrium structures. An inspection of Table II points out the following trends:

(i) In both radicals the C1C2 bond length involving the radical center is shortened while the C2C3 bond length is lengthened with respect to the values in the parent molecules. This effect is significantly more pronounced in the case of bicyclobutyl. On the other hand, the C1C4 bond length is essentially identical in the bicyclobutyl radical and in the parent molecule.

(ii) In agreement with previous theoretical studies<sup>46–48</sup> the CH bond length at the radical center (C2H2) is significantly shortened with respect to its value in the parent molecules.

(iii) The equilibrium geometries of both radicals are characterized by significantly pyramidal radical centers, the out of plane angle ( $\theta$ ) in cyclopropyl being intermediate be-

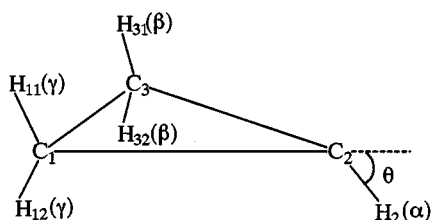
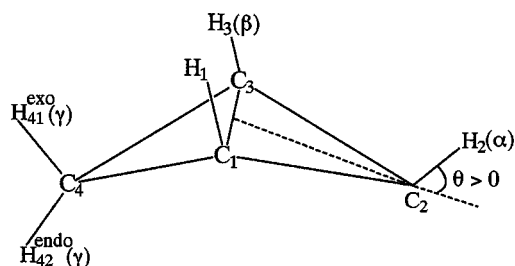


FIG. 2. Structure and atom labeling of cyclopropyl radical.

FIG. 3. Structure and atom labeling of bicyclobutyl radical in its *exo* form.

tween the *endo* and *exo* forms of bicyclobutyl. This is not surprising taking into account that bicyclobutyl radical is formed by a cyclopropane fused with a cyclopropyl ring. Together with the shortening of all the CC bond lengths, extension of the basis set leads to a reduction of the  $\theta$  angle. As we shall see, although the effect is relatively small, it can be quite significant for some hyperfine splittings.

The above three effects are connected to each other and directly derive from the modification of electronic characteristics induced by hydrogen abstraction. In terms of localized orbitals repulsion between an unpaired electron and a bonding electron pair is lower than repulsion between two bonding electron pairs. As a consequence in the radicals the pyramidity of the carbon atom is reduced and the associated CCC angle is increased, resulting in a lengthening of the opposite bond length C1C3. At the same time the hybrid orbitals of C2 forming the different bonds have more *s* character than in the parent molecule, so that C1C2, C2C3, and C2H2 bond lengths are reduced. This is confirmed by the fact that these bond lengths increase reducing the pyramidity at the radical center (see Table II), i.e., further increasing the *s* character of C2 bonding hybrid orbitals.

The energy barrier ( $\Delta E^\ddagger$ ) governing inversion at the radical center in cyclopropyl is particularly important since it determines the possibility of freezing inversion in the time scale of ESR experiments. The computed values (see Table III and Ref. 14) show a relatively low sensitivity to inclusion of correlation, whereas basis set extension leads to more sizeable effects. Our best value is obtained using UMP2/TZ2Pf geometries and the following composite procedure:  $\Delta E^\ddagger = \Delta E^\ddagger(\text{QCISD}/\text{TZP}^+) - \Delta E^\ddagger(\text{MP2}/\text{TZP}^+) + \Delta E^\ddagger(\text{MP2}/$

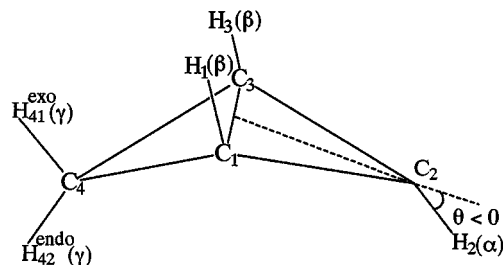
FIG. 4. Structure and atom labeling of bicyclobutyl radical in its *endo* form.

TABLE II. Geometrical parameters (Å and degrees) for cyclopropyl and bicyclobutyl radicals. See Figs. 2–4 for the atom labeling.

Cyclopropyl radical					Bicyclobutyl radical				
Parameter	UMP2/DZP		UMP2/TZ2Pf		Parameter	<i>exo</i> form		<i>endo</i> form	
	$C_S$ min.	$C_{2V}$ TS	$C_S$ min.	$C_{2V}$ TS		UMP2/DZP	UMP2/TZ2Pf	UMP2/DZP	UMP2/TZ2Pf
C1C2	1.482	1.467	1.468	1.453	C1C2	1.468	1.456	1.467	1.453
C1C3	1.538	1.549	1.529	1.539	C1C3	1.589	1.568	1.571	1.551
C1H11	1.085	1.087	1.082	1.084	C1C4	1.505	1.497	1.508	1.501
C1H12	1.085	1.087	1.082	1.084	C2H2	1.085	1.081	1.085	1.080
C2H2	1.081	1.074	1.077	1.070	C3H3	1.082	1.078	1.080	1.077
HCH	114.77	114.27	114.64	114.16	C4H41	1.087	1.083	1.088	1.084
$\theta$	42.40	0.00	39.52	0.00	C4H42	1.087	1.083	1.088	1.084
					C1C2C3	65.51	65.13	64.75	64.51
					C2C3H3	128.81	129.30	128.25	128.86
					H41C4H42	115.17	115.30	114.93	115.09
					$\theta$	48.44	47.44	−34.19	−30.90

TZ2Pf)=11.6–12.5+11.3=10.4 kJ mol<sup>−1</sup>. In agreement with previous computations the *endo* conformation of bicyclobutyl is significantly less stable than the *exo* form (Table IV). The energy difference between the two forms is increased with respect to the Hartree–Fock value (19.5 kJ mol<sup>−1</sup> at the UHF/DZP level) but is rather insensitive to the basis set ( $\Delta E$ =28.0, 28.5, and 28.5 kJ mol<sup>−1</sup> at the UMP2/DZP, UMP2/TZP<sup>+</sup>, and UMP2/TZ2Pf levels) and to inclusion of correlation energy above the simple MP2 level treatment ( $\Delta E$ =28.5 and 25.6 kJ mol<sup>−1</sup> at the UMP2/TZP<sup>+</sup> and UQCISD/TZP<sup>+</sup> levels, respectively). These values are large enough to prevent any significant role of the *endo* structure at not too high temperatures, thus confirming the assignment of the ESR spectrum at −170 °C only to the *exo* structure.

### A. Hyperfine coupling constants

The protonic ESR spectrum of cyclopropyl at 77 K shows a small negative  $\alpha$ -hydrogen hfs (−6.7 G), and four equivalent positive  $\beta$ -hydrogen hfs (+23.5 G).<sup>49,50</sup> Furthermore there are no significant variations in the spectrum at least up to 220 K.<sup>51</sup> Finally substitution by <sup>13</sup>C indicates that the  $\alpha$  carbon has a large hfs (95.9 G at 203 K).<sup>51</sup> In general, terms the small magnitude of the  $\alpha$ -hydrogen hfs and the

large magnitude of the  $\alpha$ -carbon hfs are in agreement with the pyramidal equilibrium structure obtained by all the computations. The negligible temperature dependence indicates that the potential governing inversion at the radical center is relatively deep.

The isotropic hyperfine splittings have been computed by different methods both at MP2/DZP and MP2/TZ2Pf geometries. The results of Table III show that UHF calculations, often employed in experimental studies to back the interpretations of the measurements, give very disappointing results. This trend can be traced back to the well known overestimation of spin polarization effects by this method. The isotropic hyperfine couplings computed by correlated methods at both equilibrium geometries are in fair agreement with experiment, the relative error being comparable for all atoms. Vibrational averaging improves the agreement between computed and experimental values except for H $\alpha$  (Table V). The net effect is to bring the hfs to values which would be obtained for  $\theta$  lower than the value of the equilibrium conformation [ $a(C2)$  decreases, whereas  $a(H2)$  increases]. As previously pointed out,<sup>30</sup> the ground state vibrational wave function is more localized inside the potential well, even under the barrier, than outside. So it introduces

TABLE III. Experimental isotropic hyperfine couplings [ $a(X)$  in Gauss] for the cyclopropyl radical are compared with those computed using different methods/basis sets (indicated in the first line of the heading) and geometries (optimized by method/basis set indicated in the second line of the heading). Inversion barriers ( $\Delta E$  in kJ mol<sup>−1</sup>) are also given.

Parameter	UHF/DZP	UMP2/DZP	UMP2/TZ2Pf	UQCISD/DZP	UQCISD/TZP <sup>+</sup>	Expt.
	UMP2/DZP	UMP2/DZP	UMP2/TZ2Pf	UMP2/DZP	UMP2/TZ2Pf	
$a(H2)$	−16.1	−5.7	−5.7	−6.1	−6.8	−6.7
$a(H31)$	22.7	23.0	25.4	22.8	25.3	
$a(H32)$	14.4	13.3	16.6	13.6	16.7	
$[a(H31)+a(H32)]/2$	18.6	18.1	21.0	18.2	21.0	23.5
$a(C2)$	150.7	116.9	103.6	117.4	108.6	95.9
$a(C3)$	−14.2	−7.3	−6.6	−8.7	−9.2	
$\Delta E^+$	15.9	16.6	11.3	15.4	11.6	

TABLE IV. Isotropic hyperfine couplings [ $a(X)$  in Gauss] and relative stability ( $\Delta E$  in  $\text{kJ mol}^{-1}$ ) of the *endo*-bicyclobutyl radical computed using different methods/basis sets (indicated in the first line of the heading) and geometries (optimized by the methods/basis sets indicated in the second line of the heading).

Parameter	UHF/DZP	UMP2/DZP	UMP2/TZP <sup>+</sup>	UMP2/TZP <sup>+</sup>	UQCISD/DZP	UQCISD/TZP <sup>+</sup>	UQCISD/TZP <sup>+</sup>
	UMP2/DZP	UMP2/DZP	UMP2/DZP	UMP2/TZ2Pf	UMP2/DZP	UMP2/DZP	UMP2/TZ2Pf
$a(\text{H2})$	1.0	11.2	12.9	9.4	10.5	12.1	8.6
$a(\text{H3})$	5.4	7.2	7.5	7.5	7.2	7.4	7.5
$a(\text{H41})$	-1.3	1.0	1.1	1.4	1.3	1.5	1.7
$a(\text{H42})$	8.1	6.0	6.4	6.1	5.7	5.9	5.6
$a(\text{C2})$	128.7	80.4	77.9	68.3	83.9	83.6	74.2
$a(\text{C3})$	-16.4	-8.0	-7.4	-7.4	-10.9	-10.8	-15.4
$a(\text{C4})$	34.2	34.2	33.9	36.0	34.0	33.6	35.6
$\Delta E$	19.5	28.0	28.7	28.5	25.3	25.7	25.6

more contributions of internal points. More quantitatively, the average value of  $|\theta|$  is about  $2^\circ$  lower than the corresponding equilibrium value. Vibrational effects are, anyway, quite small in view of the significant value of the vibrational frequency for inversion at the radical center. This explains the good agreement between experimental and static theoretical computations. Furthermore, the negligible temperature dependence observed experimentally is related to the negligible population, in the range of temperatures examined, of excited vibrational states. As previously reported,<sup>14</sup> at higher temperatures ( $>250$  K) sizeable effect would be detected especially for the radical carbon atom.

In the case of bicyclobutyl radical the experimental proton spectrum of 24 lines shows a doublet ( $a=12.64$  G) of triplets ( $a=4.40$  G), further split into two doublets ( $a=7.85$  and  $0.81$  G).<sup>52</sup> The couplings were initially assigned to  $\alpha, \beta, \gamma$  *endo* and  $\gamma$  *exo* protons, respectively.<sup>52</sup> Recent computations strongly suggest, however, an inversion of the assignments for  $\alpha$  and  $\gamma$  *endo* protons.<sup>53</sup>

The results of Table VI show that once again UHF calculations are unreliable. All the correlated methods give for the *exo* conformation couplings of  $H_\beta$  and  $H_\gamma^{\text{exo}}$  close to experiment. It is noteworthy that the computed hfs of  $H_\gamma^{\text{exo}}$  is negative, as previously observed in bicyclic nitroxide radicals.<sup>15(a)</sup> The situation is more involved for the remaining hydrogen hfs, since all the computations give  $a(H_\gamma^{\text{endo}}) > a(H_\alpha)$ , thus reversing the assignment suggested in Ref. 52. The original assignment was based on an out-of-plane angle near  $15^\circ$ , which gives the best agreement between computed<sup>52,54</sup> and experimental hfs, but with the constraint

that, as is normally the case, the  $\alpha$  coupling is larger than both the  $\gamma$  ones. Relaxing this constraint, the hfs computed at  $\theta \sim 45^\circ$  are in good agreement with experiment when reversing the assignment of  $\alpha$  and *endo* hfs. Moreover, a small  $\alpha$ -hfs is in agreement with the results discussed above for cyclopropyl radical.

It is noteworthy that the  $\alpha$  and  $\gamma$  hfs, although not the  $\beta$  hfs, computed for the *endo* conformation (Table IV) are also compatible with the observed ESR spectrum, but in this case a strong long-range coupling is observed only for the *exo* proton. Furthermore, the  $\alpha$  coupling is larger than both the  $\gamma$  ones. However, as mentioned above, the computed energy difference between *endo* and *exo* structures is large enough to exclude any significant role of the *endo* radical in the experimental spectrum. On the other hand, local vibrational averaging effects within the potential well corresponding to the *exo* form could be significant. Our computations (see Table V) give a strong effect for the radical carbon atom, but relatively low contributions for hydrogen atoms. The reduction of the  $\alpha$  coupling gives further support to our assignment of the experimental spectrum, whereas the hyperfine splittings of the other hydrogen atoms remain essentially unmodified.

Further insight in the origin of our results can be gained taking into account that isotropic hfs can be decomposed into the direct contribution ( $a_{\text{SOMO}}$ ) of the nominally unpaired orbital and a spin-polarization contribution ( $a_{\text{SP}}$ ) coming from correlation effects.<sup>11-13</sup> The first term can be obtained from restricted open-shell (ROHF) computations, whereas spin-polarization (together with other dynamic correlation

TABLE V. Comparison between experimental and computed (static and vibrationally averaged) isotropic hfs (in gauss).

	Static <sup>a</sup>	Cyclopropyl vibr.aver. <sup>b</sup>	Expt.	Static <sup>a</sup>	Bicyclobutyl vibr.aver. <sup>b</sup>	Expt.
$C_\alpha$	108.6	101.4	95.9	124.9	119.9	
$C_\beta$	-9.2	-9.6		12.2	12.3	
$H_\alpha$	-6.8	-8.9	-6.7	5.2	3.6	7.9
$H_\beta$	21.0 <sup>c</sup>	21.8 <sup>c</sup>	23.5	2.2	2.7	4.4
$H_\gamma^{\text{exo}}$				-1.0	-1.1	$\pm 0.8$
$H_\gamma^{\text{exo}}$				10.1	10.0	12.6

<sup>a</sup>TZP<sup>+</sup>/QCISD/UMP2/TZ2Pf.

<sup>b</sup>Vibrational contributions from UMP2/DZP computations.

<sup>c</sup>Mean value between syn and anti protons.

TABLE VI. Experimental isotropic hyperfine couplings (in gauss) for the *exo*-bicyclobutyl radical are compared with those computed using different methods/basis sets (indicated in the first line of the heading) and geometries (optimized by method/basis set indicated in the second line of the heading).

Atom	UHF/DZP UMP2/DZP	UMP2/DZP UMP2/DZP	UMP2/TZP <sup>+</sup> UMP2/DZP	UMP2/TZP <sup>+</sup> UMP2/TZPf	UQCISD/DZP UMP2/DZP	UQCISD/TZP <sup>+</sup> UMP2/DZP	UQCISD/TZP <sup>+</sup> UMP2/TZ2Pf	Expt.
H2	-2.0	6.4	7.9	6.6	5.0	6.4	5.2	7.8 or 12.6
H3	-1.7	2.4	2.6	1.9	2.9	3.0	2.2	4.4
H41	-0.8	-1.5	-1.6	-1.7	-0.9	-0.9	-1.0	±0.8
H42	7.6	9.7	10.2	10.0	9.6	10.3	10.1	12.6 or 7.8
C2	160.8	132.7	128.6	123.5	132.8	129.7	124.9	
C3	5.5	13.5	13.9	12.1	13.5	14.3	12.2	
C4	4.8	5.4	5.9	7.7	4.2	4.3	6.3	

effects) is simply the difference between UQCISD and ROHF results. Furthermore the interpretation of the results will be based on a localized picture in which the unpaired electron is initially located on a hybrid orbital of the radical carbon atom, and delocalization occurs (together spin polarization) through interactions with the appropriate CH bonds (see Fig. 5). It must be stressed that valence bond calculations of the transmission of the hyperfine splitting through localized bonds via a spin polarization mechanism result in an alternating sign of the hfs along the chain<sup>55,56</sup> (see Fig. 6). In agreement with earlier *ab-initio* computations,<sup>17</sup> our results confirm this trend for the radical center and for  $\alpha$  protons, but show that this simple rule does not always apply for more distant protons: as a matter of fact the spin polarization contribution for these atoms can be positive, negative, or negligible depending on the out of plane angle  $\theta$  (see Figs. 7–9).

Of course, the primary effect of pyramidalization is to bring the localized carbon orbital containing most of the unpaired electron from a nearly pure  $p$  to an  $sp^n$  hybrid with increasing contributions from the  $2s$  orbital. This modification strongly increases the isotropic hfs on C2.<sup>14,30</sup> Also the coupling constants on  $\alpha$ -hydrogen atoms are very sensitive to the pyramidalization of the radical center (Fig. 7). As a matter of fact the negative coupling found for  $\theta=0^\circ$  is almost entirely due to spin polarization (see Fig. 7) and becomes positive at  $|\theta|>30^\circ$  as a consequence of the rapid increase of the delocalization of the SOMO on  $\alpha$ -hydrogens. The trend is the same in both radicals, although the curve becomes slightly asymmetric in the case of bicyclobutyl due to the asymmetric placement of the second cyclopropane ring.

For the  $\beta$  hydrogens the point to be underlined is that the isotropic hfs decrease with  $\theta$  more rapidly for the proton *syn* to the unpaired electron (Fig. 8). This means that in the bicyclobutyl radical lower  $\beta$  hfs are found for *exo* structure

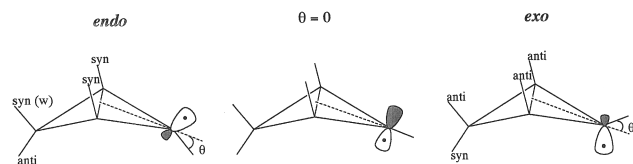


FIG. 5. Relative orientations of the localized orbital nominally containing the unpaired electron and the various hydrogen atoms for different structures of the bicyclobutyl radical.

than for *endo* one. Thus the presence of an exocyclic ring does not alter the general trend, but reduces the absolute values of  $\beta$  protons. Note that experimental examples of inequivalent hfs are known for  $\beta$  protons in the bicyclo [2.2.1]heptane series.<sup>15,16,57,58</sup> They have been interpreted as consistent with a pyramidal geometry around the radical site with a bending of the  $CH\alpha$  bond toward the *endo*  $\gamma$  proton.<sup>15(a),16</sup> As mentioned above, long-range hfs are expected to be usually very small. By analogy with NMR results,<sup>59</sup> the few strong positive long-range hfs have been ascribed to a  $W$ -planar arrangement of the bonds between the  $\gamma$  proton and the  $p$ -orbital nominally containing the unpaired electron (Fig. 5). Straightforward application of this rule would indicate that only for a planar or *endo* equilibrium structure a strong  $\gamma$  hfs would be observed, corresponding to the *exo* proton.

Our results show a quite different pattern. In the most stable *exo* conformation the  $CH\alpha$  bond is bent toward the  $\gamma$ -*exo* proton (H41), so that no  $W$  arrangement can be found for any  $\gamma$ -proton and the  $W$  rule does not apply. The *endo*- $\gamma$  hfs is the largest one, with a positive spin-polarization contribution (6.22 G) approximately double than the direct SOMO contribution (3.42 G). The *exo*- $\gamma$  hfs is negative with a vanishing SOMO contribution. As the  $\theta$  angle decreases, both SOMO and spin polarization contributions decrease for the *endo*- $\gamma$  proton, whereas both contributions increase for the *exo*- $\gamma$  proton. In the  $\theta \sim 0^\circ$  conformation, a naive application of the  $W$  rule would result in an incorrect attribution of the largest  $\gamma$  hfs to the *exo* proton, whereas our computations found the largest positive hfs on the *endo* proton (see Fig. 9), which is in a *syn* position with respect to the carbon  $p$  orbital (Fig. 5). The hfs on the two  $\gamma$  protons become

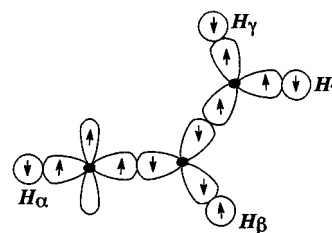


FIG. 6. Spin polarization contributions to short- and long-range isotropic hfs.

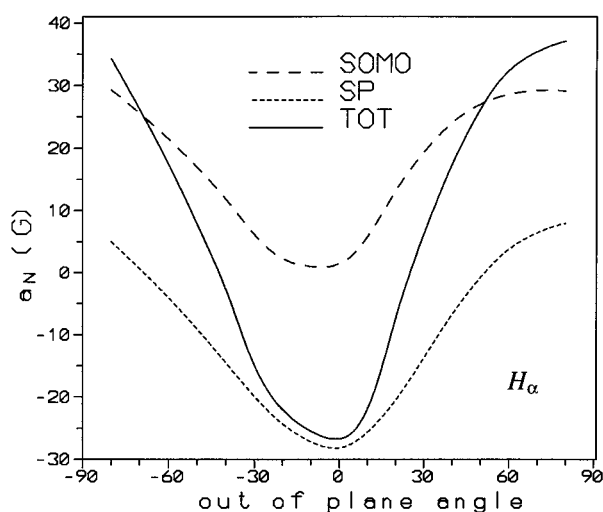


FIG. 7. Evolution of isotropic hfs on  $\alpha$  protons as a function of the out of plane angle  $\theta$  (see Figs. 2, 3) in bicyclobutyl radical.

identical (and small) at  $\theta \sim -20^\circ$ . Next a strong positive contribution of spin polarization is found again on the *syn* atom in the secondary minimum found for the *endo* conformation. In this case the result is in agreement with the *W* rule, which applies to the *exo*- $\gamma$  proton.

This analysis shows that a large positive spin polarization contribution is only found for the  $\gamma$  proton involved in a CH bond *syn* to the carbon orbital containing the unpaired electron, whereas this term is negative for an *anti* arrangement. Since the SOMO contribution is always positive and is also larger for a *syn* arrangement, some sort of *syn* rule appears more general than the more customary *W* rule. This rule apply equally well to *endo* and *exo* forms of bicyclobutyl, but requires that the C $\beta$ -C $\gamma$  bond does not lie in the

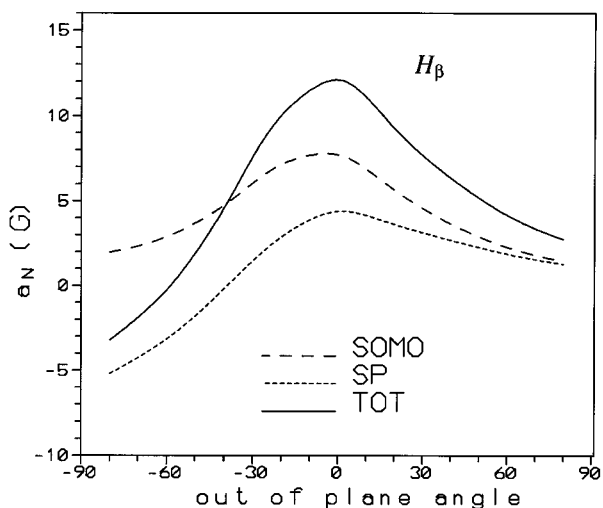


FIG. 8. Evolution of isotropic hfs on  $\beta$  protons as a function of the out of plane angle  $\theta$  (see Figs. 2, 3) in bicyclobutyl radical.

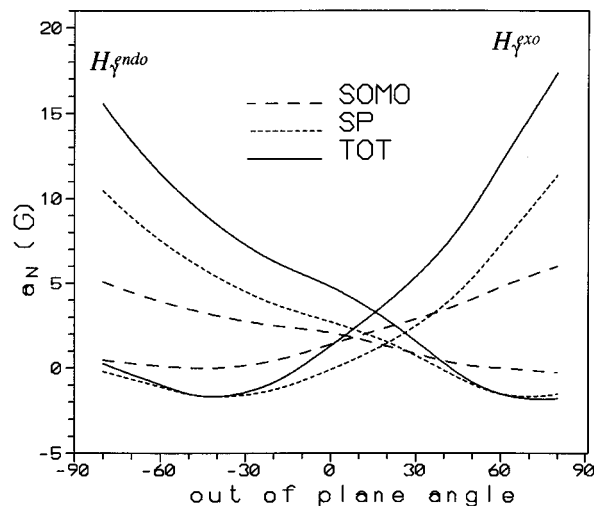


FIG. 9. Evolution of isotropic hfs on  $\gamma$  protons as a function of the out of plane angle  $\theta$  (see Figs. 2, 3) in bicyclobutyl radical.

nodal plane of the carbon orbital containing most of the unpaired electron.

#### IV. CONCLUSION

We have analyzed the structural and magnetic characteristics of two representative strained radicals, and have found that our computational protocol performs remarkably well. Extended basis sets provides structures, harmonic force fields, and hyperfine data of nearly chemical accuracy. Furthermore vibrational averaging effects cannot be neglected for quantitative work. More generally our results confirm that hyperfine interactions are critically dependent on stereochemical conditions, which can, in some case, lead to a counterintuitive ordering of short- and long-range couplings. In particular, our theoretical work leads us to conclude that strong long-range isotropic hfs are found for protons respecting a “*syn* rule” rather than the well known “*W* rule.” The new rule seems to apply without restrictions for  $\beta$  protons and for  $\gamma$  protons provided that the C $\beta$ -C $\gamma$  bond does not lie in the nodal plane of the carbon orbital containing most of the unpaired electron.

In summary, completely *ab-initio* studies offer a powerful additional tool for the characterization and interpretation of the physicochemical properties of free-radicals when only partial data are available or concurrent interpretations are possible.

<sup>1</sup>G. T. Babcock, M. K. El-Deeb, P. O. Sandusky, M. M. Whittaker, and J. W. Whittaker, *J. Am. Chem. Soc.* **114**, 3727 (1992).

<sup>2</sup>V. Volker, A. F. Wagner, M. Frey, F. A. Neugebauer, and J. Knappe, *Proc. Natl. Acad. U.S.A.* **89**, 996 (1992).

<sup>3</sup>E. Mulliez, M. Fontecave, J. Gaillard, and P. Reichard, *J. Biol. Chem.* **268**, 2296 (1993).

<sup>4</sup>V. Bachler and K. Hildebrand, *Rad. Phys. Chem.* **40**, 59 (1992).

<sup>5</sup>T. J. Stone, T. Buckman, P. L. Nordio, and H. McConnell, *Proc. Natl. Acad. Sci. U.S.A.* **54**, 1010 (1965).

<sup>6</sup>*Spin Labeling*, Vols. 1 and 2, edited by L. D. Berliner (Academic New York, 1976, 1979).



- <sup>7</sup>E. G. Rozantsef, *Free Nitroxyl Radicals* (Plenum, New York, 1970).
- <sup>8</sup>J. F. Keana, *Chem. Rev.* **78**, 37 (1978).
- <sup>9</sup>A. Cogne, A. Grand, P. Rey, and R. Subra, *J. Am. Chem. Soc.* **111**, 3230 (1989).
- <sup>10</sup>A. Caneschi, D. Gatteschi, and P. Rey, *Prog. Inorg. Chem.* **39**, 331 (1991).
- <sup>11</sup>Y. Ellinger, A. Rassat, R. Subra, and G. Berthier, *J. Am. Chem. Soc.* **95**, 2372 (1973).
- <sup>12</sup>Y. Ellinger, A. Rassat, R. Subra, and G. Berthier, *J. Chem. Phys.* **62**, 1 (1975).
- <sup>13</sup>Y. Ellinger, A. Rassat, R. Subra, G. Berthier, and Ph. Millie, *Chem. Phys. Lett.* **11**, 362 (1971).
- <sup>14</sup>V. Barone, C. Minichino, H. Faucher, R. Subra, and A. Grand, *Chem. Phys. Lett.* **205**, 324 (1993).
- <sup>15</sup>(a) J. Gloux, M. Guglielmi, and H. Lemaire, *Mol. Phys.* **19**, 833 (1970); (b) R. Marx and L. Bonazzola, *ibid.* **19**, 899 (1970); (c) P. Bakusis, J. K. Kochi, and P. J. Krusic, *J. Am. Chem. Soc.* **92**, 1434 (1970); (d) T. Kawamura, T. Koyama, and T. Yonezawa, *ibid.* **95**, 3220 (1973).
- <sup>16</sup>Y. Ellinger, B. Levy, Ph. Millie, and R. Subra, in *Localization and Delocalization in Quantum Chemistry*, edited by O. Chalvet (Reidel, Dordrecht, 1975).
- <sup>17</sup>Y. Ellinger, R. Subra, B. Levy, Ph. Millie, and G. Berthier, *J. Chem. Phys.* **62**, 10 (1975).
- <sup>18</sup>F. W. King, *Chem. Rev.* **76**, 157 (1976).
- <sup>19</sup>(a) H. Sekino, and R. J. Bartlett, *J. Chem. Phys.* **82**, 4225 (1985); (b) S. A. Pereira, J. D. Watts, and R. J. Bartlett, *ibid.* **100**, 1425 (1994).
- <sup>20</sup>I. Carmichael, *J. Phys. Chem.* **95**, 6198 (1991).
- <sup>21</sup>D. Feller, E. D. Glendening, E. A. McCullough, Jr., and R. J. Miller, *J. Chem. Phys.* **99**, 2829 (1993).
- <sup>22</sup>B. Fernández, P. Jørgensen, E. A. McCullough, Jr., and J. Symons, *J. Chem. Phys.* **99**, 5995 (1993).
- <sup>23</sup>(a) B. Engels, *J. Chem. Phys.* **100**, 1380 (1994); (b) H. U. Suter and B. Engels, *ibid.* **100**, 2936 (1994).
- <sup>24</sup>V. Barone, C. Adamo, A. Grand, Y. Brunel, M. Fontecave, and R. Subra, *J. Am. Chem. Soc.* **117**, 1083 (1995).
- <sup>25</sup>M. J. Frisch, G. W. Trucks, M. Head-Gordon, P. M. W. Gill, M. W. Wong, J. B. Foresman, B. G. Johnson, H. B. Schlegel, M. A. Robb, E. S. Replogle, R. Gomperts, J. L. Andres, K. Raghavachari, J. S. Binkley, C. Gonzalez, R. L. Martin, D. J. Fox, D. J. DeFrees, J. Baker, J. J. P. Stewart, and J. A. Pople, GAUSSIAN92 (Gaussian Inc., Pittsburgh, 1992).
- <sup>26</sup>V. Barone, P. Jensen, and C. Minichino, *J. Mol. Spectrosc.* **154**, 252 (1992).
- <sup>27</sup>(a) C. Minichino and V. Barone, *J. Chem. Phys.* **100**, 3717 (1994); (b) V. Barone, and C. Minichino, *Theochem.* **330**, 365 (1995).
- <sup>28</sup>J. A. Pople, M. Head-Gordon, and K. Raghavachari, *J. Chem. Phys.* **87**, 5968 (1987).
- <sup>29</sup>C. J. Cramer and M. H. Lim, *J. Phys. Chem.* **98**, 5024 (1994).
- <sup>30</sup>V. Barone, C. Minichino, A. Grand, and R. Subra, *J. Chem. Phys.* **99**, 6787 (1993).
- <sup>31</sup>S. Huzinaga *J. Chem. Phys.* **42**, 293 (1965).
- <sup>32</sup>T. H. Dunning, Jr. *J. Chem. Phys.* **90**, 1007 (1989).
- <sup>33</sup>T. H. Dunning and P. J. Hay, *Modern Theoretical Chemistry* (Plenum, New York, 1986), pp. 1–28, Chap. 1.
- <sup>34</sup>T. H. Dunning, Jr., *J. Chem. Phys.* **90**, 1007 (1989).
- <sup>35</sup>D. M. Chipman, *Theor. Chim. Acta* **76**, 73 (1989); *J. Chem. Phys.* **54**, 55 (1989).
- <sup>36</sup>K. Fukui, *J. Phys. Chem.* **74**, 4161 (1970); *Acc. Chem. Res.* **14**, 363 (1981).
- <sup>37</sup>W. H. Miller, N. C. Handy, and J. E. Adams, *J. Chem. Phys.* **72**, 99 (1980).
- <sup>38</sup>C. Zhixing, *Theor. Chim. Acta* **75**, 481 (1989).
- <sup>39</sup>P. Gemaschi, *Mol. Phys.* **40**, 401 (1980).
- <sup>40</sup>J. L. Duncan and G. R. Burns, *J. Mol. Spectrosc.* **30**, 253 (1969).
- <sup>41</sup>R. J. Butcher and W. J. Jones, *J. Mol. Spectrosc.* **47**, 64 (1973).
- <sup>42</sup>K. W. Cox, M. D. Harmony, G. Nelson, and K. B. Wiberg, *J. Chem. Phys.* **50**, 1976 (1976).
- <sup>43</sup>K. B. Wiberg, S. T. Waddell, and R. E. Rosenberg, *J. Am. Chem. Soc.* **112**, 2184 (1990).
- <sup>44</sup>J. Pacanski and M. Yoshimine, *J. Phys. Chem.* **89**, 1880 (1985).
- <sup>45</sup>K. A. Nguyen and M. S. Gordon, *J. Am. Chem. Soc.* **117**, 3835 (1995).
- <sup>46</sup>(a) M. Yoshimine and J. Pacansky, *J. Chem. Phys.* **74**, 5168 (1981); (b) J. Pacansky and J. S. Chang, *ibid.* **74**, 5539 (1981).
- <sup>47</sup>J. Pacansky and M. Dupuis, *J. Am. Chem. Soc.* **104**, 419 (1982).
- <sup>48</sup>J. Pacansky and A. Gutierrez, *J. Phys. Chem.* **87**, 3074 (1983).
- <sup>49</sup>R. W. Fessenden and R. H. Schuler, *J. Chem. Phys.* **39**, 2147 (1963).
- <sup>50</sup>K. S. Chen, D. G. Edge, and G. K. Kochi, *J. Am. Chem. Soc.* **95**, 7036 (1973).
- <sup>51</sup>L. J. Johnston and K. U. Ingold, *J. Am. Chem. Soc.* **108**, 2343 (1986).
- <sup>52</sup>P. J. Krusic, J. P. Jesson, and J. K. Kochi, *J. Am. Chem. Soc.* **91**, 4566 (1969).
- <sup>53</sup>V. Barone, C. Adamo, A. Grand, and R. Subra, *Chem. Phys. Lett.* **246**, 53 (1995).
- <sup>54</sup>Y. Ellinger, R. Subra, and G. Berthier, *J. Am. Chem. Soc.* **100**, 4961 (1978).
- <sup>55</sup>Z. Luz, *J. Chem. Phys.* **48**, 4186 (1968).
- <sup>56</sup>M. Barfield, *J. Phys. Chem.* **74**, 621 (1968).
- <sup>57</sup>T. Kawamura, T. Koyama, and T. Yonezawa, *J. Am. Chem. Soc.* **92**, 7222 (1970).
- <sup>58</sup>T. Kawamura, Y. Sugiyama, and T. Yonezawa, *Mol. Phys.* **33**, 1499 (1977).
- <sup>59</sup>(a) J. Meinwald and A. Lewis, *J. Am. Chem. Soc.* **83**, 2769 (1961); (b) A. Rassat, C. W. Jeford, J. M. Lehn, and B. Waegell, *Tetrahedron Lett.* **5**, 233 (1964); (c) S. Sternhell, *Quarterly Rev.* **23**, 236 (1969).